Current Biology

Specializations in optic flow encoding in the pretectum of hummingbirds and zebra finches

--Manuscript Draft--

Manuscript Number:	CURRENT-BIOLOGY-D-21-00763R2
Full Title:	Specializations in optic flow encoding in the pretectum of hummingbirds and zebra finches
Article Type:	Report
Corresponding Author:	Douglas Altshuler University of British Columbia Vancouver, CANADA
First Author:	Graham Smyth
Order of Authors:	Graham Smyth
	Vikram Baliga
	Andrea Gaede
	Douglas Wylie
	Douglas Altshuler
Abstract:	All visual animals experience optic flow - global visual motion across the retina, which is used to control posture and movement1. The midbrain circuitry for optic flow is highly conserved in vertebrates2–6, and these neurons show similar response properties across tetrapods4,7–16. These neurons have large receptive fields and exhibit both direction- and velocity-selectivity in response to large moving stimuli. Hummingbirds deviate from the typical vertebrate pattern in several respects17,18. Their lentiformis mesencephali (LM) lacks the directional bias seen in other tetrapods and has an overall bias for faster velocities. This led Ibbotson19 to suggest that the hummingbird LM may be specialized for hovering close to visual structures, such as plants. In such an environment, even slight body motions will translate into high velocity optic flow. A prediction from this hypothesis is that hummingbird LM neurons should be more responsive to large visual features. We tested this hypothesis by measuring neural responses of hummingbirds and zebra finches to sine wave gratings of varying spatial and temporal frequencies. As predicted, the hummingbird LM displayed an overall preference for fast optic flow because neurons were biased to lower spatial frequencies. These neurons were also tightly tuned in the spatiotemporal domain. We found that the zebra finch LM specializes along another domain: many neurons were initially tuned to high temporal frequencies followed by a shift in location and orientation to slower velocity tuning. Collectively, these results demonstrate that the LM has distinct and specialized tuning properties in at least two bird species.
Additional Information:	
Question	**Response**
Standardized datasets A list of datatypes considered standardized under Cell Press policy is available here. Does this manuscript report new standardized datasets?	No
Original Code Does this manuscript report original code?	No

Graphical Abstract

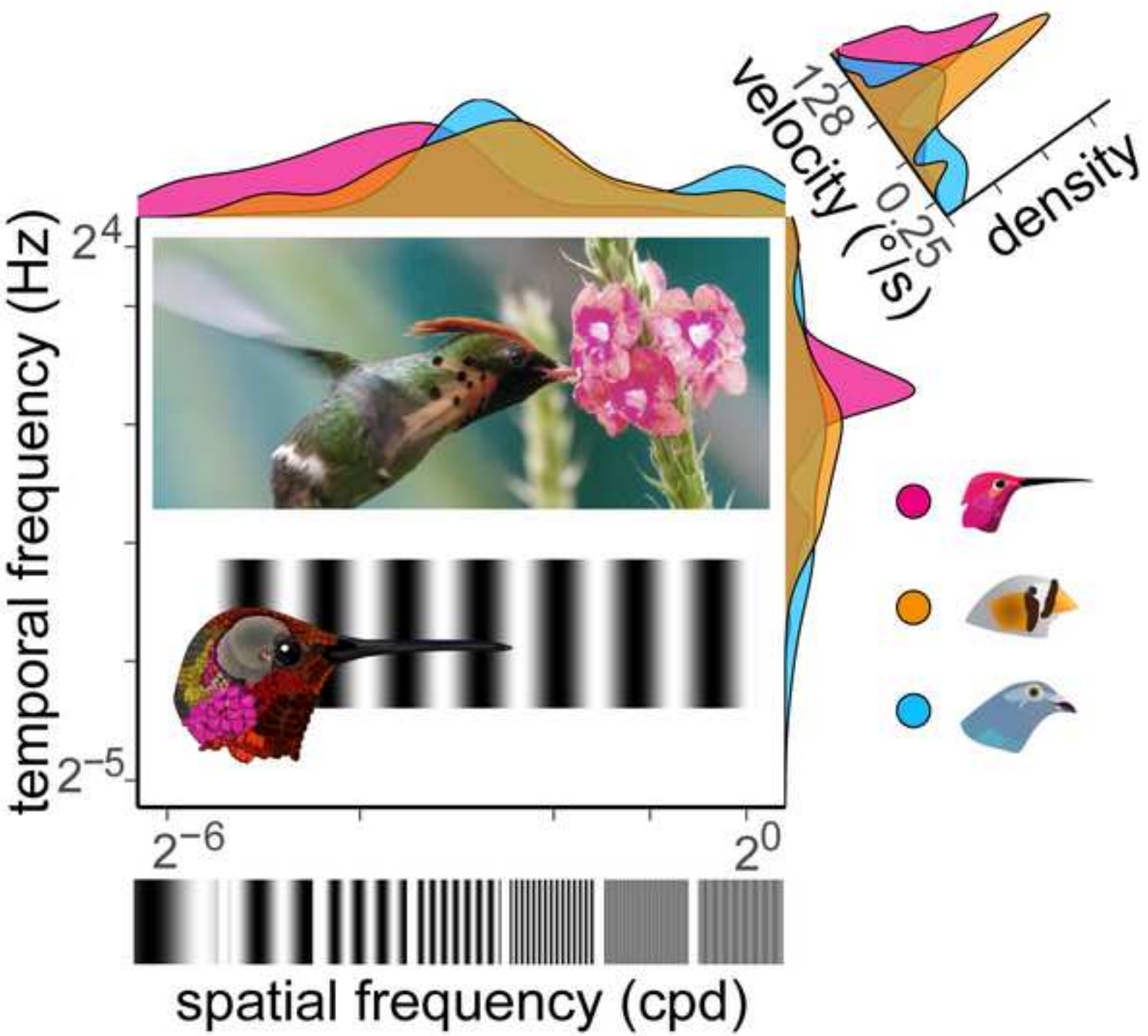

Specializations in optic flow encoding in the pretectum of hummingbirds and zebra finches

Graham Smyth[1,4], Vikram B. Baliga[1,4], Andrea H. Gaede[1,2,3,4], Douglas R. Wylie[2,5], and Douglas L. Altshuler[1,5,6]

[1]Department of Zoology, University of British Columbia, 4200-6270 University Blvd., Vancouver, BC, V6T 1Z4, Canada

[2]Department of Biological Sciences, University of Alberta, CW 405 Biological Sciences Bldg., Edmonton, AB, T6G 2E9, Canada

[3]Structure and Motion Laboratory, Royal Veterinary College, University of London, Hatfield, AL9 7TA, United Kingdom

[4]These authors contributed equally

[5]Senior authors

[6]Lead contact

Keywords: avian flight, electrophysiology, visual motion, visual neuroscience

Summary

All visual animals experience optic flow - global visual motion across the retina, which is used to control posture and movement[1]. The midbrain circuitry for optic flow is highly conserved in vertebrates[2–6], and these neurons show similar response properties across tetrapods[4,7–16]. These neurons have large receptive fields and exhibit both direction- and velocity-selectivity in response to large moving stimuli. Hummingbirds deviate from the typical vertebrate pattern in several respects[17,18]. Their lentiformis mesencephali (LM) lacks the directional bias seen in other tetrapods and has an overall bias for faster velocities. This led Ibbotson[19] to suggest that the hummingbird LM may be specialized for hovering close to visual structures, such as plants. In such an environment, even slight body motions will translate into high velocity optic flow. A prediction from this hypothesis is that hummingbird LM neurons should be more responsive to large visual features. We tested this hypothesis by measuring neural responses of hummingbirds and zebra finches to sine wave gratings of varying spatial and temporal frequencies. As predicted, the hummingbird LM displayed an overall preference for fast optic flow because neurons were biased to lower spatial frequencies. These neurons were also tightly tuned in the spatiotemporal domain. We found that the zebra finch LM specializes along another domain: many neurons were initially tuned to high temporal frequencies followed by a shift in location and orientation to slower velocity tuning. Collectively, these results demonstrate that the LM has distinct and specialized tuning properties in at least two bird species.

Results and Discussion

In tetrapods, optic flow is analyzed by two visual pathways in the midbrain. In birds, the retinal-recipient nuclei in these circuits are called the nucleus lentiformis mesencephali (LM) of the pretectal pathway, and the nucleus of the basal optic root (nBOR) of the accessory optic system[20,21]. LM and nBOR are homologs of the nucleus of the optic tract (NOT) and the terminal nuclei in mammals, respectively[2–4]. The majority of LM and NOT neurons prefer temporal-to-nasal motion in the contralateral visual field[7–13]. We previously found that the hummingbird LM lacked a unidirectional bias, and showed a distribution of preferred directions suggesting a uniform distribution[18]. The current study also required directional tuning analysis prior to experiments in the spatiotemporal domain. Thus, we were able to combine new measurements of directional tuning preferences in hummingbirds and zebra finches with our previous data set[18]. The pigeon data, included for comparison, are archival[22–24]. Direction tuning was measured by recording neuron firing rates in response to dotfield stimuli (Fig. 1A). Each dot pattern was moved in one of eight directions (45° steps), in random order and with four sweeps per direction. The pattern was moved for five seconds, with a five second pause before shifting to the next direction. Pigeons and zebra finches (Fig. 1C,D) show the pattern of tetrapods from all vertebrate classes: the majority of neurons prefer temporal-to-nasal motion such that there is a strong population bias for this direction (Fig. 1E). For hummingbirds (Fig. 1B), the distribution of preferred directions is now bimodal with most neurons preferring either temporal-to-nasal direction or a downward nasal-to-temporal direction. Although this distribution is different from our previous finding, there is still no overall unitary directional bias in the population given the distribution of peak locations and the shapes of the tuning curves (Fig. 1E, Fig. S1).

We next measured the spatiotemporal tuning of LM neurons from hummingbirds and zebra finches, which were compared with archival data from pigeons[22–24]. Spatiotemporal tuning is measured using drifting sine wave gratings of varying spatial and temporal frequency (SF,TF) in the preferred direction. The ratio of TF to SF is velocity. In our previous study, which used dotfield stimuli, we found that hummingbird LM neurons generally preferred fast stimuli (>40°/sec). With the dotfield stimuli, the maximum velocity we could use was 80°/sec, to which some neurons

were responding maximally[18]. A distinct advantage of sine wave gratings is that we were able to extend the maximum tested velocities from 80 up to 1032°/sec.

We tested zebra finch neurons at six spatial frequencies (0.031-1 cycles per degree [cpd]) and six temporal frequencies (0.031-16 Hz), which matches the range used for most pigeon neurons from archival data. In our initial recordings of hummingbirds, we again found that some neurons preferred very fast velocities, which was evident by these neurons responding maximally to 0.031 cpd. We therefore added one lower spatial frequency stimulus (0.0155 cpd) for hummingbirds. In total, we recorded 72 LM neurons from the hummingbird, 75 from the zebra finch, and compared these to 61 LM neurons from archival pigeon data[22–25]. The responses of a representative hummingbird LM neuron to gratings moving in the preferred direction are shown in figure 1F-H. To determine the peak location, orientation and range of neural responses, we fit two-dimensional Gaussian functions[26]. The best-fit Gaussian for this representative neuron is depicted in figure 1I.

Given that we have previously shown that hummingbird LM neurons are more tightly tuned to velocity using random dot patterns[18], we reasoned that these neurons should also be more tightly tuned in the spatiotemporal domain. The best-fit 2D Gaussians for representative LM neurons from each species are shown (Fig. 1J-L). Some neurons had two peak response regions in the spatiotemporal domain. This has also been observed for some NOT (LM homolog) neurons in the wallaby[9] and for nBOR neurons of hummingbirds, zebra finches, and pigeons[17]. For neurons with two peaks, we only analyzed the primary peak, which had the higher maximal spike rate. Some peaks were located at the edges of the sampled spatiotemporal space (open circles in Fig. 2A). For Gaussians with peaks located within the sampling space, we quantified tightness of tuning by calculating the volume under the Gaussian fit (see equation 8, methods). LM neurons are more tightly tuned in hummingbirds (5-95% CI = 12-14 log Hz x log cpd) than in zebra finches (CI = 15-17), which are more tightly tuned than LM neurons of pigeons (CI = 20-23) (Fig. 1M).

In a separate study, we performed a spatiotemporal analysis of nBOR[17], the midbrain nucleus in the accessory optic system that also encodes optic flow. However, unlike the LM, which in non-hummingbird species has a bias for temporal-to-nasal (regressive) optic flow, nBOR neurons prefer one of the other three cardinal directions of optic flow: up, down, or nasal-to-temporal (progressive). The same distribution of direction preferences was confirmed for the hummingbird nBOR. The hummingbird nBOR also had a distribution of velocity preferences that fully overlapped with zebra finches and pigeons. The only feature of the hummingbird nBOR that differed compared to the other species was that the neurons were more tightly tuned in the spatiotemporal domain.

We next asked if differences in velocity preferences among species[18] were due to differences in preference for spatial and/or temporal frequency. Preference was determined as the location of the peak of the best-fit 2D Gaussian for each neuron (Fig. 2A). For this analysis, the edge cases were included because the peak locations would correspond to the edge or even more extreme values. We fit linear mixed models to determine species-wise effects. Hummingbird LM neurons preferred much faster velocities (5-95% CI = 27.30-55.71°/sec) than zebra finches (CI = 7.36-15.03°/sec) or pigeons (CI = 4.20-9.06°/sec) (Fig. 2B). Hummingbird LM neurons also exhibited a substantial preference for lower spatial frequencies (5-95% CI =0.05-0.08 cpd) compared to zebra finches (CI = 0.13-0.21 cpd) and pigeons (CI = 0.18-0.30 cpd) (Fig. 2C). Differences in temporal frequency, were more modest but hummingbirds (5-95% CI = 2.01-3.12 Hz) showed a preference for higher temporal frequencies compared to pigeons (CI = 1.11-1.77 Hz) but not more than zebra finches (CI = 1.46-2.22 Hz) (Fig. 2D). Overall, these results support a prediction of Ibbotson's[19] ecological hypothesis: hummingbird LM neurons prefer faster velocities because they are tuned to lower spatial frequencies. Such a preference confers high sensitivity to nearby objects such as leaves and branches when hovering or flying through dense foliage to reach

flowers or insect prey[27]. These objects have a large retinal image size and high velocity during self-motion due to proximity.

The orientation of the 2D Gaussians can also be used to determine if a given cell is tuned to a specific velocity (diagonally oriented) or tuned to a specific temporal frequency (horizontally oriented), termed "spatiotemporally independent". Following Priebe et al.[26], we used partial correlation methods to determine if cells showed a significant velocity orientation or were significantly spatiotemporally independent. This was done by fitting two additional 2D Gaussian models, a velocity oriented prediction and a spatiotemporally independent prediction by constraining the Q parameter (see equation 3) to 0 and -1, respectively. We then computed the partial correlations of the real data with each of the two predictions to determine whether the neuronal response was closer to the velocity-oriented prediction (R_{vel}) or spatiotemporally independent prediction (R_{ind}) (equations 4,5).

Contour plots of neural responses from one zebra finch (Fig. 3A) and one hummingbird (Fig. 3F) neuron are compared to Gaussians constrained to Q=0 (velocity oriented; Fig. 3B,G) and Q=-1 (spatiotemporally independent; Fig. 3C,H). A cell that is velocity oriented will exhibit different temporal frequency peaks at each spatial frequency (Fig. 3D), but alignment for every spatial frequency at a specific velocity (Fig. 3E). In contrast, a spatiotemporally independent neuron will show alignment at a specific temporal frequency (Fig. 3I) instead of a velocity (Fig. 3J). We have purposely chosen representative cases to illustrate a zebra finch neuron oriented to velocity and a hummingbird neuron oriented to temporal frequency.

The partial correlation analysis revealed that for all three species, some neurons are velocity oriented, some are spatiotemporally independent (TF oriented), and some are unclassifiable (Fig. 3K). The last category arose for cells in which R_{vel} and R_{ind} were roughly equivalent or for cells in which neither R_{vel} nor R_{ind} were statistically significant. There was a significant difference in cell orientation classes among species (χ^2 test, $p < 0.001$) such that zebra finches have more velocity oriented and fewer independent cells (Fig. 3L). Moreover, the 5-95% credible interval for R_{vel} was higher for zebra finches (0.42-0.55) than for both hummingbirds (0.26-0.38) and pigeons (0.07-0.21) (Fig. 3M). The 5-95% credible interval for R_{ind} was lower for zebra finches (0.32-0.45) than for pigeons (0.49-0.63).

It was unexpected that zebra finch LM neurons would have such a strong bias for velocity-oriented over spatiotemporally independent neuron classes. It has previously been noted that motion detecting cells can have different tuning in response to motion stimulus between an initial transient phase and a subsequent steady-state phase[28–30]. Thus, the difference in tuning among species led us to ask if tuning preferences differed between initial and sustained responses. We performed an analysis of peristimulus histogram bin size, which indicated that there is often a higher burst of activity in the first 40-200 ms following stimulus onset (Fig. 4A-F). This initial transient phase was compared to a steady-state phase of 1000-2000 ms following stimulus onset.

We first asked if the spatiotemporal preference changed from the transient to the steady-state response. The number of cells in this analysis was reduced, in hummingbirds from 61 to 47 and in zebra finches from 75 to 69. This reduction occurred because some of the transient response data could not be reliably fit with a 2D Gaussian ($R^2 < 0.5$), which at least in some cases was due to asymmetric responses[31]. The locations of the Gaussian peaks (Fig. 4G,H) did not change substantially for hummingbird LM neurons (SF: $T_{46} = 0.37$, $p = 0.72$; TF: $T_{46} = 1.17$, $p = 0.25$; velocity: $T_{46} = 1.07$, $p = 0.29$), but exhibited a marked shift downwards on the temporal frequency versus spatial frequency plot for zebra finches (SF: $T_{68} = 3.20$, $p = 0.002$; TF: $T_{68} = 9.37$, $p <$

0.001). This downward shift to lower velocity (T_{68} = 9.26, $p < 0.001$) was primarily driven by excitation by lower temporal frequencies as neural responses reached steady state.

We next asked if the orientations of the Gaussians changed between the initial transient and steady-state phases, which would be indicated by a shift in velocity (R_{vel}) and independent (R_{ind}) correlations (Fig. 4I,J). The number of cells was further reduced to 22 in hummingbirds and to 45 for zebra finches, because we only analyzed cells for which neither the initial nor the steady-state Gaussians were edge cases. Changes in hummingbird LM neurons were modest such that the overall distribution of tuning orientation classes were similar (Fig. 4K; χ^2 test, $p = 0.62$). For zebra finches, the majority of cells were initially sensitive to temporal frequency, but at steady state the overall distribution shifted such that there was a strong preference for velocity orientation (χ^2 test, $p < 0.001$).

Previous studies showed that most neurons in pigeon LM[32] and wallaby NOT[33] were oriented to temporal frequency rather than to velocity. Moreover, the few velocity-oriented cells are typically "slow" cells, preferring velocities less than 4°/s. This association was also found in the pigeon nBOR, which has more slow neurons and more velocity oriented cells[25,32]. Hummingbirds and zebra finches deviate from this pattern in that both have more velocity oriented LM neurons, and in that their cells generally encode faster velocities.

What are the potential functions of these different classes of spatiotemporally tuned cells? Ibbotson et al.[9] emphasized that fast optic flow neurons are important for detection of the first 50-100 ms at the onset of self-motion when retinal slip velocity is high and the system is operating in an open-loop state[34,35]. After this initial phase, the retinal image is relatively stable in the closed-loop phase and any retinal slip would be detected by the slow neurons. Zebra finches seem to have a taken a slightly different approach. Most of the neurons prefer faster velocities, are oriented to temporal frequency during stimulus onset, but oriented to stimulus velocity during the steady-state phase. Thus, these neurons could function during both the initial open-loop and the closed-loop phases of the optokinetic response. We also note that the overall population of zebra finches relatively tightly tuned to a velocity around 16°/s (Fig. 2A,B), which may reflect some visual signal that is pertinent to their environment but remains currently unknown. Hummingbirds seem to have taken markedly different approach to encoding optic flow. They have a hypertrophied LM[36], prefer faster velocities, and we show here that they also have much narrower tuning and are tuned to lower spatial frequencies. These properties should facilitate the impressive ability of hummingbirds to change both speed and direction[37], i.e., their maneuverability[38–40], as they would often be operating in an open-loop mode. Given the results of spatiotemporal tuning across even just the few species of birds that have now been examined, it is clear that there is considerable diversity in what was previously thought to be a highly conserved circuit for optic flow processing.

Acknowledgements: This research was funded by Project Grant PJT-169033 from the Canadian Institutes of Health Research. Graphical abstract credits: Brent Sinclair (photo); Sylvia Heredia (hummingbird).

Author Contributions: DLA, DRW, GS, and AHG conceived the study. GS, AHG, and DRW collected the data. VBB, GS, and DRW performed the data analysis. DLA, DRW, VBB, GS, and AHG wrote and edited the manuscript.

Competing interests: The authors declare no competing interests.

Main figures titles and legends

Figure 1. Neurons in the hummingbird lentiformis mesencephali (LM) are narrowly tuned in the spatiotemporal domain. A) A dotfield stimulus was moved randomly in each of eight directions to determine direction preference. B-D) Polar histograms of direction vectors for all directionally tuned neurons are shown for hummingbirds (magenta), zebra finches (orange), and pigeons (blue). Directions are indicated as (u)p, (d)own, (t)emporal, and (n)asal. E) Normalized tuning curves for all neurons are plotted in polar coordinates. Thick lines indicate median values, which indicate a strong nasal bias for pigeons and zebra finches but not for hummingbirds. F) Sine-wave gratings of varying spatial frequency (SF) were moved at different velocities (and thus different temporal frequencies [TF]) to measure spatiotemporal tuning. G) Peristimulus time histograms (PSTHs) are shown for a representative hummingbird LM neuron to each SF/TF combination. PSTHs are averages of 4 sweeps, 2 s long (20 ms bins). These data are represented by a contour plot (H), fit with a 2-dimensional Gaussian (I). J-L) Representative Gaussian fits of four LM neurons from each species. M) Spatiotemporal tuning width is defined as the volume under the Gaussian fit and shows a clear hierarchy: pigeons are the most broadly tuned and hummingbirds are the most narrowly tuned in the spatiotemporal domain. Black borders indicate cells displayed in J-L. Black circles indicate cells displayed in figure 3A-J. See also figure S1

Figure 2. Hummingbird LM neurons prefer faster velocities because they are tuned to lower spatial frequencies. (A) The locations of the peaks of the unconstrained best-fit Gaussians are plotted by species. For neurons with two peaks, only the location of the larger peak is depicted. Unfilled circles indicate that fitted Gaussians were found to have peaks at or beyond the edge of the investigated ranges of spatial and/or temporal frequencies. Kernel density estimates for the spatial frequency, temporal frequency, and velocity are plotted above, to the right, and in the upper right, respectively. (B – D) Distributions of species' effects in models of velocity, spatial frequency, and temporal frequency (see Table S1). In each panel, the species' mean effect is indicated by the black dot, whereas the 5-95% credible interval (CI) is shown using a black bar. See also Table S1.

Figure 3. Neurons in the zebra finch LM exhibit a greater tendency for velocity as opposed to temporal frequency orientation. A contour plot of a zebra finch neuron (A) is compared to a 2D Gaussian fitted of the data to the velocity-oriented (B) and independent prediction (C). R^2 values indicate goodness of fit for each Gaussian prediction. Line plots depict mean firing rate versus stimulus velocity (D) and temporal frequency (E). F-J) Same analysis for a representative hummingbird neuron. K) Scatter plot showing the partial correlations of best-fit 2D Gaussians of the velocity-oriented model (R_{vel}) versus the spatiotemporally independent model (R_{ind}) for all cells. The location of each point indicates the extent to which an individual neuron is velocity-oriented (upper left) or spatiotemporally independent (lower right). The black lines represent the criteria cutoff for cells to be classified as velocity-oriented, unclassified, or spatially independent. L) Bar graphs showing the percentage of cells in each category by species. M) Distributions of species' effects in models of R_{vel} and R_{ind} (see Table S2). The species' mean effect is indicated by the black dot, whereas the 5-95% credible interval (CI) is shown using a black bar. See also Table S2.

Figure 4. Zebra finch LM neurons respond initially to high temporal frequencies (TF) and are TF-oriented, but then shift over time to velocity orientation at lower TF. Differences between initial transient and steady-state responses can be viewed by averaging the normalized PSTHs for all hummingbird (A, magenta) and zebra finch (B, orange) cells. Data are displayed for the full two seconds of stimulus motion. C) Representative raw PSTHs from one hummingbird and one zebra finch cell are shown at distinct TF-SF combinations. Baseline firing rates to a non-moving stimulus are indicated by the dashed lines. Initial transient (IT) and steady-state (SS) phases are indicated by rectangles. For the zebra finch neuron in C, the best-fit Gaussians for the full sweep

(FS, 2s) of stimulus motion (D), the initial transient (40-200 ms, E), and the steady-state (1000-2000 ms, F) response are shown. Scatterplots (G) and boxplots (H) show shifts in the peak locations of the Gaussians from the initial transient (grey) to steady-state (colored) responses, revealing that zebra finch LM neurons are initially responsive to higher temporal frequencies. Grey lines connect individual cells in which at least one phase had peak response at the edge of the stimulus region. Black lines connect cells without edge cases. "*" indicates statistical significance at $P<0.05$. I,J) Shifts in the partial correlations show that zebra finches are initially oriented to temporal frequency (high R_{ind}) and then shift to velocity orientation (high R_{vel}) during steady state response. K) Distributions of cell orientation for initial transient and steady-state responses show a stronger shift for zebra finches than hummingbirds.

STAR Methods

RESOURCE AVAILABILITY

Lead contact: Further information and requests for resources and reagents should be directed to and will be fulfilled by the lead contact, Douglas L. Altshuler (doug.altshuler@ubc.ca).

Materials availability: This study did not generate new unique reagents.

Data and code availability: All spike-sorted electrophysiological data and analysis code are available via Figshare (https://doi.org/10.6084/m9.figshare.19425737).

EXPERIMENTAL MODEL AND SUBJECT DETAILS

Electrophysiological recordings were made from 15 adult male Anna's hummingbirds (*Calypte anna*) and 21 adult male zebra finches (*Taeniopygia guttata*). All procedures were approved by the University of British Columbia Animal Care Committee in accordance with the guidelines set out by the Canadian Council on Animal Care.

METHOD DETAILS

Electrophysiological measurements: Stereotaxic surgeries were performed using a custom-built frame for both hummingbirds and zebra finches (Herb Adams Engineering, Glendora, CA, USA). Zebra finch coordinates were determined from Nissl-stained sections and additional information from Mark Konishi's unpublished zebra finch brain atlas. Hummingbird coordinates were determined entirely from our own sections. For anesthesia, an intramuscular injection of ketamine/xylazine (65 mg/kg ketamine / 8 mg/kg xylazine) was delivered to the pectoralis major, and supplemental injections were delivered as needed. A subcutaneous injection of 0.9% saline was provided prior to surgery. The head was angled downwards at an angle 45° to the horizontal plane. A small exposure through the skull and dura mater overlying the right telencephalon allowed vertical access to the LM.

Recordings were made using glass microelectrodes (5 µm tip diameter) filled with 2M NaCl. The extracellular signals were amplified (x10,000), bandpass filtered (0.1-3 kHz), and acquired at 50 kHz using a CED (Cambridge, UK) micro1401-3. Prior to running stimulus presentation programs, we first identified LM neurons by their characteristic spontaneous activity and strong response to visual motion in their preferred direction and (in most cases) suppression in their anti-preferred ("null") direction. This initial search was performed by moving a large handheld stimulus, made of white cardboard with black patterns.

Once we found a well isolated cell, a gaming computer monitor (144 Hz, 1920 × 1080 pixels, ASUS VG248QE) was positioned 30 cm from the bird's contralateral eye and within the cell's receptive field. The monitor occupied an ~84° X 53° (width X height) area of the bird's visual field. Two stimulus programs were used, one to identify a cell's direction preference, and a second to measure that cell's spatiotemporal tuning in the preferred and anti-preferred directions. The direction tuning program produced a dotfield stimulus made of 250 randomly positioned black dots (2.1° diameter) on a white background. The stimulus was moved at a velocity of 12.6°/s in one of 8 randomly assigned directions, 45° apart (see Figure 1A). Each direction was tested with at least four sweeps lasting 4 s with 4 s pauses between each sweep. Each change in visual stimulus triggered TTL pulse sent from the stimulus computer to the recording computer, which ran Spike2 for Windows (Version 8, CED; Cambridge, UK).

The spatiotemporal tuning program produced 42 combinations of sinusoidal black and white gratings with spatial frequencies ranging from 0.0155 to 1.0 cycles/degree (cpd) and temporal

frequencies ranging from 0.031 to 16 cycles/s (Hz). Drifting gratings were presented in randomized order and lasted for 2s and were followed by a 2s pause. Four sweeps were recorded for each spatial frequency/temporal frequency combination.

Recording sites were confirmed using a dextran injection (Dextran Texas Red™ 3000MW, or Dextran micro-Emerald 3000MW, ThermoFisher Scientific) at the end of each experiment. Animals were euthanized via a lethal dose of ketamine/xylazine mixture and then transcardially perfused with 0.9% saline followed by 4% paraformaldehyde.

QUANTIFICATION AND STATISTICAL ANALYSIS

Spike sorting: Raw neural data were processed offline first using the spike sorting algorithm in Spike 2 (CED, Cambridge, UK) to identify single units. We used trigger thresholds and a sliding window to identify individual spikes that were then matched to full-wave templates for spike classification. We set the template window parameters to include the full spike amplitude and grouped similar templates post-hoc using principal component data and an overdraw function that enabled visual inspection of individual spikes coded by template. Spike sorted data were next analyzed using custom scripts in Matlab (R2017a; MathWorks; Natick, MA).

Analysis of direction tuning: Each cell's firing rate at each stimulus direction was calculated as the average of four sweeps and plotted in polar coordinates. This was compared to the cell's spontaneous firing rate during paused visual stimulus. We next used Rayleigh's test for uniformity to determine if the cell's firing rate was uniform across all direction, i.e., not directionally modulated. For cells that were non-uniform ($P < 0.05$), the preferred direction was calculated as the mean vector:

$$Preferred\ direction = \tan^{-1}\left(\frac{\sum_n (FR_n \times \sin\theta_n)}{\sum_n (FR_n \times \cos\theta_n)}\right) \quad (1)$$

where *FR* = firing rate and *n* = stimulus motion direction in radians. Any cells in which the ratio of the response to the preferred relative to the anti-preferred direction was less than 150% were excluded.

We asked if the LM population direction tuning differed by species by calculating the median direction tuning curve for each of hummingbirds, zebra finches, and pigeons. Cubic splines with degrees of freedom varying from 5 to 20 were fit to normalized data and the best fitting spline was determined using the second-order Akaike Information Criterion. The median response value across cells was calculated across all directions and separately for each species.

Analysis of spatiotemporal tuning: Cumulative peristimulus time histograms (PSTHs; 20 bins) were generated across all four sweeps for each combination of spatial and temporal frequency stimuli. The PSTH mean firing rates (minus the spontaneous rate) were then used to generate each cell's spatiotemporal contour plot. Spatiotemporal tuning was described by the peak and volume of this surface of the 2D best-fit Gaussian on a logarithmic scale. Priebe et al.[26] defined the Gaussian function as:

$$G(sf, tf) = A \times e^{\frac{-\left(log_2(sf) - log_2(sf_0)\right)^2}{{\sigma_{sf}}^2}} \times e^{\frac{-\left(log_2(tf) - log_2\left(tf_p(sf)\right)\right)^2}{{\sigma_{tf}}^2}} \quad (2)$$

where:

$$tf_p(sf) = 2^{(Q+1)\times\left(log_2(sf) - log_2(sf_0)\right) + \log_2(tf_0)} \quad (3)$$

where A is the z-axis amplitude, and sf and tf are the spatial and temporal frequencies, respectively, of the specific grating pattern. sf_0 the peak value along the spatial frequency axis and tf_0 is the peak value along the temporal frequency axis. The spread of the function is described by σ_{sf} and σ_{tf} in the spatial and temporal frequency domains, respectively. Q is the slope of the relationship between a cell's preferred velocity and spatial frequency.

We fit Gaussian functions using the Microsoft Excel solver function and the R package gaussplotR[41]. To maximize goodness of fit, we optimized values of all parameters (sf_0, tf_0, σ_{sf}, σ_{tf}, and Q), which is the "unconstrained" best-fit model. Goodness of fit was assessed using R^2 value between the Gaussian model fit and the raw data. To determine whether a cell was "velocity oriented" or "spatiotemporally independent", we fit two additional Gaussian models with constrained Q parameters. For a truly independent cell, the slope of that plot, and thus Q, is -1, meaning the velocity preference is strongly dependent on spatial frequency. In contrast, for a truly velocity oriented cell, Q is 0 because a plot of velocity versus spatial frequency would have a slope of zero. To determine whether each cell's tuning was better described by the velocity-oriented or spatiotemporally independent predictions, we computed partial correlations of raw data with the simulated responses[42]:

$$R_{ind} = \frac{(r_i - r_s \times r_{is})}{\sqrt{(1 - {r_s}^2)(1 - {r_{is}}^2)}} \quad (4)$$

$$R_{vel} = \frac{(r_s - r_i \times r_{is})}{\sqrt{(1 - {r_i}^2)(1 - {r_{is}}^2)}} \quad (5)$$

where R_{ind} and R_{vel} are partial correlations, r_i and r_s are the correlations of the raw data with the independent- and velocity-oriented predictions, respectively. r_{is} is the correlation of the independent prediction with the velocity-oriented prediction. Fisher Z-transforms were used to determine the statistical significance of each of R_{ind} and R_{vel} as:

$$Z_f = \frac{1}{2} \times ln\left(\frac{1 + R}{1 - R}\right) \quad (6)$$

where Z_f is the z-score of either R_{ind} or R_{vel}, and R is the corresponding partial correlation coefficient. To classify cells as independently- or velocity-oriented, we then computed differences between the corresponding z-scores:

$$Z_{diff} = \frac{Z_{f,ind} - Z_{f,vel}}{\sqrt{\left(\frac{1}{N_{ind} - 3}\right) + \left(\frac{1}{N_{vel} - 3}\right)}} \quad (7)$$

where $Z_{f,ind}$ and $Z_{f,vel}$ are the Fisher Z-transform for R_{ind} and R_{vel}, and $N_{ind} = N_{vel}$ = the number of sine-wave gratings used in the best-fit 2D Gaussian. After [43], a p-value of 0.1 corresponds to an absolute Z_{diff} of 1.65 and was chosen to denote significance. Cells were considered unclassifiable if the Z_{diff} values were between -1.65 and 1.65. Spatiotemporally independent cells were classified as those having $Z_{diff} \geq 1.65$ and $R_{ind} >> 0$. Velocity-oriented cells were defined as those with $Z_{diff} \leq -1.65$ and $R_{vel} >> 0$.

To measure the breadth of tuning in the spatiotemporal domain, we calculated the volume under the normalized Gaussian surface as:

$$2 * \pi * \sqrt{|\sigma_{sf}|} * \sqrt{|\sigma_{tf}|} \quad (8)$$

For the PSTH analysis in figure 4A,B, each cell's mean firing rate (minus the spontaneous rate) was normalized to its cells maximum firing rate along each of 200 bins (10 ms bin size). Data were then averaged by species for each temporal-frequency/spatial frequency combination.

Hypothesis testing: Statistical analyses were performed using R (v4.1.2). Many details of statistical tests, including all sample sizes, are provided in the main text and figures legends. For hypothesis testing related to analyses shown in figures 1-3, we asked whether species identity explained variance in each of: volume under the Gaussian fit, location of spatiotemporal peaks (on plots of temporal frequency vs. spatial frequency), and Gaussian orientation. For each of these dependent variables, we fit Bayesian generalized linear mixed models[44] and used a normal prior for fixed effects. Adjustments to parameters of the prior did not meaningfully affect results (code available on Figshare repository). We then determined statistical significance by assessing whether the 5-95% credible intervals (CIs) of fixed effects overlapped.

In LM neurons of pigeons[24], NOT neurons of wallabies[9], and nBOR neurons of hummingbirds zebra finches, and pigeons[17], cells clustered into "fast" and "slow" groups, with the dividing line at 4°/s. The density kernel plots of velocity (Fig. 2A) did not show any evidence of this divide, so we performed all analyses for the full population of hummingbirds and zebra finch neurons. The same approach was used with the archival pigeon data for consistency.

For hypothesis testing related to comparing initial transient and steady state data, we used two-sided paired t-tests to account for repeated measures from the same cell. Comparison with pigeons was not possible because temporally-resolved responses were not available. Dependent variables included: log(velocity), SF peak location, and TF peak location. We subsequently applied Bonferroni corrections to p-values to mitigate the effects of multiple hypothesis testing.

References

1. Gibson, J.J. (1954). The visual perception of objective motion and subjective movement. Psychol Rev *61*, 304–314.

2. Fite, K.V. (1985). Pretectal and accessory-optic visual nuclei of fish, amphibia and reptiles: theme and variations. Brain Behav Evol *26*, 71–80.

3. McKenna, O.C., and Wallman, J. (1985). Accessory optic system and pretectum of birds: comparisons with those of other vertebrates. Brain Behav Evol *26*, 91–116.

4. Simpson, J.I. (1984). The accessory optic system. Annu Rev Neurosci *7*, 13–41.

5. Voogd, J., and Wylie, D.R.W. (2004). Functional and anatomical organization of floccular zones: a preserved feature in vertebrates. J Comp Neurol *470*, 107–112.

6. Weber, J.T. (1985). Pretectal complex and accessory optic system of primates (part 1 of 2). Brain Behav Evol *26*, 117–128.

7. Collewijn, H. (1975). Direction-selective units in the rabbit's nucleus of the optic tract. Brain Res *100*, 489–508.

8. Fan, T.X., Weber, A.E., Pickard, G.E., Faber, K.M., and Ariel, M. (1995). Visual responses and connectivity in the turtle pretectum. J Neurophysiol *73*, 2507–2521.

9. Ibbotson, M.R., Mark, R.F., and Maddess, T.L. (1994). Spatiotemporal response properties of direction-selective neurons in the nucleus of the optic tract and dorsal terminal nucleus of the wallaby, *Macropus eugenii*. J Neurophysiol *72*, 2927–2943.

10. Hoffmann, K.-P., and Schoppmann, A. (1981). A quantitative analysis of the direction-specific response of neurons in the cat's nucleus of the optic tract. Exp Brain Res *42*, 146–157.

11. Manteuffel, G. (1984). Electrophysiology and anatomy of direction-specific pretectal units in *Salamandra salamandra*. Exp Brain Res *54*, 415–425.

12. Winterson, B.J., and Brauth, S.E. (1985). Direction-selective single units in the nucleus lentiformis mesencephali of the pigeon (*Columba livia*). Exp Brain Res *60*, 215–226.

13. Mustari, M.J., and Fuchs, A.F. (1990). Discharge patterns of neurons in the pretectal nucleus of the optic tract (NOT) in the behaving primate. J Neurophysiol *64*, 77–90.

14. Soodak, R.E., and Simpson, J.I. (1988). The accessory optic system of rabbit. I. Basic visual response properties. J Neurophysiol *60*, 2037–2054.

15. Rosenberg, A.F., and Ariel, M. (1990). Visual-response properties of neurons in turtle basal optic nucleus in vitro. J Neurophysiol *63*, 1033–1045.

16. Morgan, B., and Frost, B.J. (1981). Visual response characteristics of neurons in nucleus of basal optic root of pigeons. Exp Brain Res *42*, 181–188.

17. Gaede, A.H., Baliga, V.B., Smyth, G., Gutiérrez-Ibáñez, C., Altshuler, D.L., and Wylie, D.R. (2022). Response properties of optic flow neurons in the accessory optic system of hummingbirds versus zebra finches and pigeons. J Neurophysiol *127*, 130–144.

18. Gaede, A.H., Goller, B., Lam, J.P.M., Wylie, D.R., and Altshuler, D.L. (2017). Neurons responsive to global visual motion have unique tuning properties in hummingbirds. Curr Biol *27*, 279–285.

19. Ibbotson, M.R. (2017). Visual neuroscience: unique neural system for flight stabilization in hummingbirds. Curr Biol *27*, R58–R61.

20. Gamlin, P.D.R., and Cohen, D.H. (1988). Retinal projections to the pretectum in the pigeon (*Columba livia*). J Comp Neurol *269*, 1–17.

21. Karten, J.H., Fite, K.V., and Brecha, N. (1977). Specific projection of displaced retinal ganglion cells upon the accessory optic system in the pigeon (*Columba livia*). Proc Nat Acad Sci USA *74*, 1753–1756.

22. Crowder, N.A., Lehmann, H., Parent, M.B., and Wylie, D.R.W. (2003). The accessory optic system contributes to the spatio-temporal tuning of motion-sensitive pretectal neurons. J Neurophysiol *90*, 1140–1151.

23. Crowder, N.A., Dickson, C.T., and Wylie, D.R.W. (2004). Telencephalic input to the pretectum of pigeons: an electrophysiological and pharmacological inactivation study. J Neurophysiol *91*, 274–285.

24. Wylie, D.R.W., and Crowder, N.A. (2000). Spatiotemporal properties of fast and slow neurons in the pretectal nucleus lentiformis mesencephali in pigeons. J Neurophysiol *84*, 2529–2540.

25. Crowder, N.A., Dawson, M.R.W., and Wylie, D.R.W. (2003). Temporal frequency and velocity-like tuning in the pigeon accessory optic system. J Neurophysiol *90*, 1829–1841.

26. Priebe, N.J., Cassanello, C.R., and Lisberger, S.G. (2003). The neural representation of speed in macaque area MT/V5. J Neurosci *23*, 5650–5661.

27. Stiles, F.G. (1995). Behavioral, ecological and morphological correlates of foraging for arthropods by the hummingbirds of a tropical wet forest. Condor *97*, 853–878.

28. Egelhaaf, M., and Borst, A. (1989). Transient and steady-state response properties of movement detectors. J Opt Soc Am A *6*, 116–127.

29. Maddess, T., and Laughlin, S.B. (1985). Adaptation of the motion-sensitive neuron H1 is generated locally and governed by contrast frequency. Proc Roy Soc B *225*, 251–275.

30. Perrone, J.A., and Thiele, A. (2002). A model of speed tuning in MT neurons. Vision Res *42*, 1035–1051.

31. Perrone, J.A. (2006). A Single mechanism can explain the speed tuning properties of MT and V1 complex neurons. J Neurosci *26*, 11987–11991.

32. Winship, I.R., Crowder, N.A., and Wylie, D.R.W. (2006). Quantitative reassessment of speed tuning in the accessory optic system and pretectum of pigeons. J Neurophysiol *95*, 546–551.

33. Ibbotson, M.R., and Price, N.S.C. (2001). Spatiotemporal tuning of directional neurons in mammalian and avian pretectum: a comparison of physiological properties. J Neurophysiol *86*, 2621–2624.

34. Cohen, B., Matsuo, V., and Raphan, T. (1977). Quantitative analysis of the velocity characteristics of optokinetic nystagmus and optokinetic after-nystagmus. J Physiol *270*, 321–344.

35. Collewijn, H. (1972). Latency and gain of the rabbit's optokinetic reactions to small movements. Brain Res *36*, 59–70.

36. Iwaniuk, A.N., and Wylie, D.R.W. (2007). Neural specialization for hovering in hummingbirds: hypertrophy of the pretectal nucleus lentiformis mesencephali. J Comp Neurol *500*, 211–221.

37. Ibbotson, M.R., Hung, Y.-S., Meffin, H., Boeddeker, N., and Srinivasan, M.V. (2017). Neural basis of forward flight control and landing in honeybees. Sci Rep *7*, 14591.

38. Dakin, R., Segre, P.S., Straw, A.D., and Altshuler, D.L. (2018). Morphology, muscle capacity, skill, and maneuvering ability in hummingbirds. Science *359*, 653–657.

39. Clark, C.J. (2009). Courtship dives of Anna's hummingbird offer insights into flight performance limits. Proc R Soc B *276*, 3047–3052.

40. Sholtis, K.M., Shelton, R.M., and Hedrick, T.L. (2015). Field flight dynamics of hummingbirds during territory encroachment and defense. PLoS ONE *10*, e0125659.

41. Baliga, V. (2021). gaussplotR: fit, predict and plot 2D-Gaussians in R. J Open Source Softw *6*, 3074.

42. Levitt, J.B., Kiper, D.C., and Movshon, J.A. (1994). Receptive fields and functional architecture of macaque V2. J Neurophysiol *71*, 2517–2542.

43. Crowder, N.A., and Wylie, D.R. (2002). Responses of optokinetic neurons in the pretectum and accessory optic system of the pigeon to large-field plaids. J Comp Physiol A *188*, 109–119.

44. Hadfield, J.D. (2010). MCMC methods for multi-response generalized linear mixed models: the MCMCglmm R package. J Stat Softw *33*, 1–22.

Supplemental References

S1. Vogels, R., and Orban, G.A. (1994). Activity of inferior temporal neurons during orientation discrimination with successively presented gratings. J Neurophysiol *71*, 1428–1451.

KEY RESOURCES TABLE

REAGENT or RESOURCE	SOURCE	IDENTIFIER
Chemicals, peptides, and recombinant proteins		
Dextran Texas Red 3000MW	ThermoFisher Scientific	
Dextran micro-Emerald 3000MW	ThermoFisher Scientific	
Ketamine (Narketan)	cdmv	118577
Xylazine	UBC Animal Care Services	N/A
Deposited data		
Data and code for the manuscript	figshare	doi
Experimental models: Organisms/strains		
Anna's hummingbird (*Calypte anna*), adult male	Wild caught	N/A
Zebra finch (*Taeniopygia gutatta*), adult male	L'Oisellerie de l'Estrie, Québec, Canada	N/A
Software and algorithms		
gaussplotR	Baliga, VB. 2021	doi:10.21105/joss.03074
Matlab	MathWorks, Natick, MA	R2017a
R	R Core Team	v4.1.2
Spike2	CED, Cambridge, UK	v8
Other		
Stereotax	Herb Adams Engineering, Glendora, CA	N/A

Figure 1

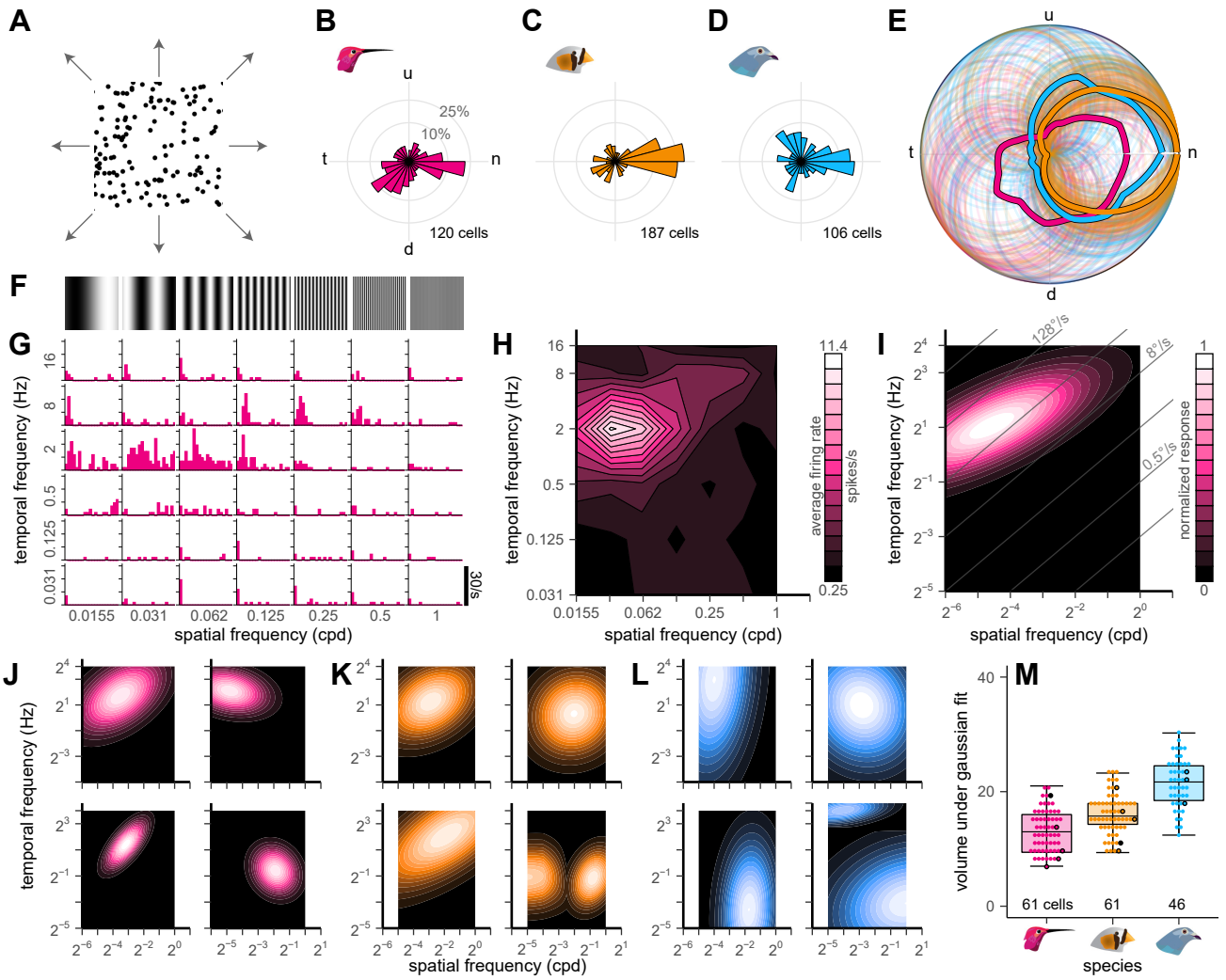
A
B
C
D
E
u
t
n
d
25%
10%
120 cells
187 cells
106 cells
F
G
temporal frequency (Hz)
16
8
2
0.5
0.125
0.031
30/s
0.0155
0.031
0.062
0.125
0.25
0.5
1
spatial frequency (cpd)
H
11.4
0.25
average firing rate
spikes/s
I
128°/s
8°/s
0.5°/s
normalized response
1
0
J
K
L
M
volume under gaussian fit
40
20
0
61 cells
61
46
species

Figure 2

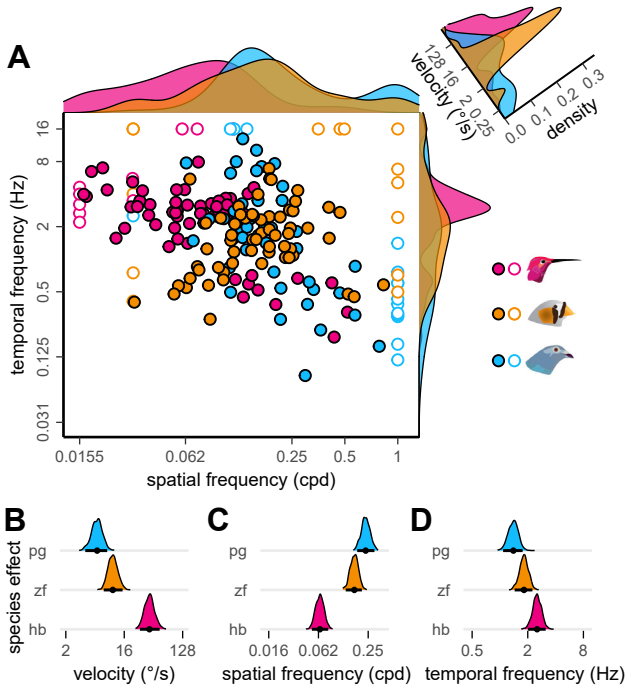
A
temporal frequency (Hz)
16
8
2
0.5
0.125
0.031
0.0155
0.062
0.25
0.5
1
spatial frequency (cpd)
velocity (°/s)
128
16
2
0.25
density
0.0
0.1
0.2
0.3
B
species effect
pg
zf
hb
2
16
128
velocity (°/s)
C
pg
zf
hb
0.016
0.062
0.25
spatial frequency (cpd)
D
pg
zf
hb
0.5
2
8
temporal frequency (Hz)

Figure 3

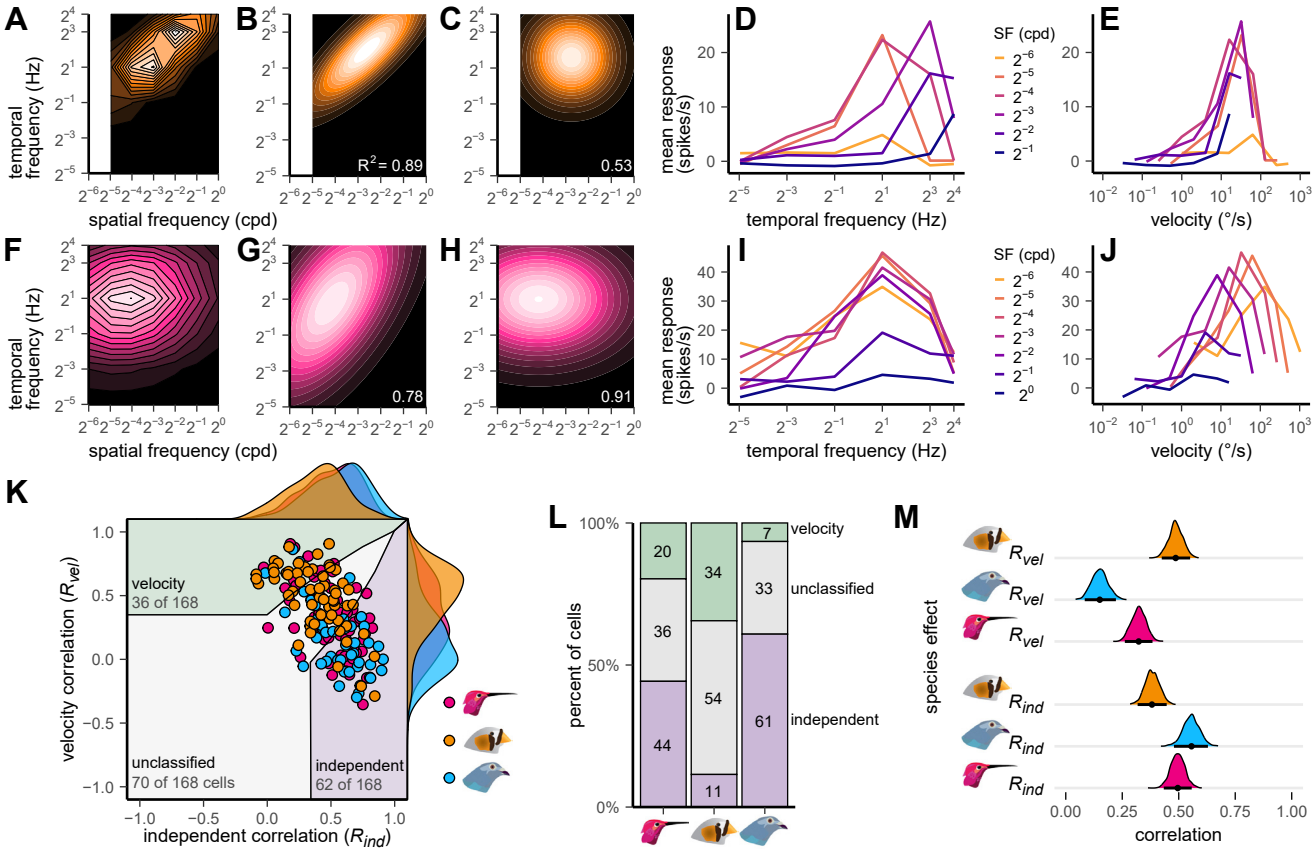
A
B
C
D
E
F
G
H
I
J
K
L
M
temporal frequency (Hz)
spatial frequency (cpd)
R² = 0.89
0.53
0.78
0.91
mean response (spikes/s)
temporal frequency (Hz)
SF (cpd)
velocity (°/s)
velocity correlation (R_vel)
independent correlation (R_ind)
velocity
36 of 168
unclassified
70 of 168 cells
independent
62 of 168
percent of cells
100%
50%
0%
20
36
44
34
54
11
7
33
61
unclassified
independent
species effect
correlation
0.00
0.25
0.50
0.75
1.00

Figure 4

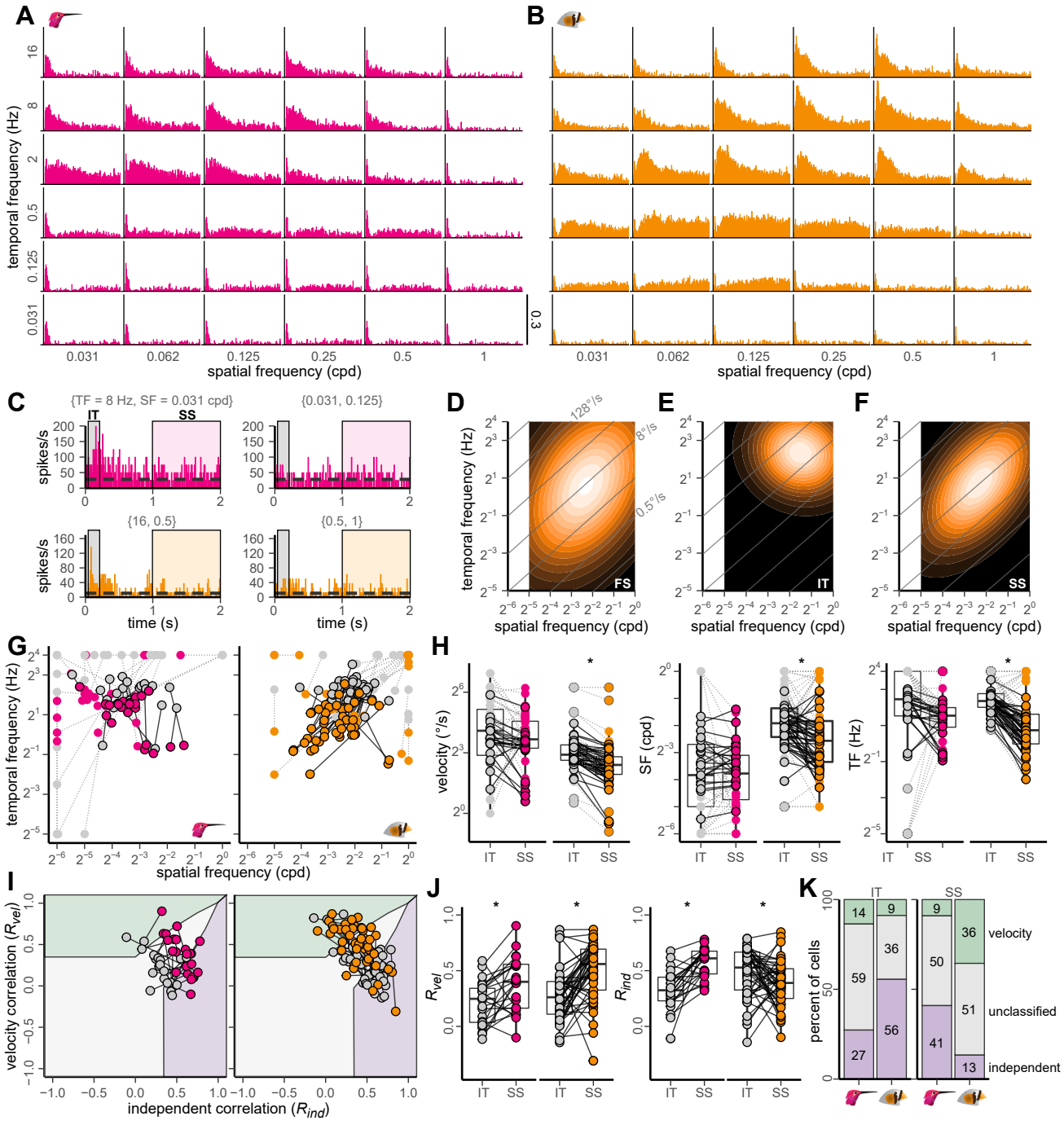
A
B
temporal frequency (Hz)
16
8
2
0.5
0.125
0.031
0.3
0.031
0.062
0.125
0.25
0.5
1
spatial frequency (cpd)
C
{TF = 8 Hz, SF = 0.031 cpd}
{0.031, 0.125}
{16, 0.5}
{0.5, 1}
IT
SS
spikes/s
time (s)
D
E
F
128°/s
8°/s
0.5°/s
FS
IT
SS
G
H
velocity (°/s)
SF (cpd)
TF (Hz)
I
velocity correlation (R_{vel})
independent correlation (R_{ind})
J
R_{vel}
R_{ind}
K
percent of cells
14
9
59
27
36
56
9
36
50
41
51
13
velocity
unclassified
independent

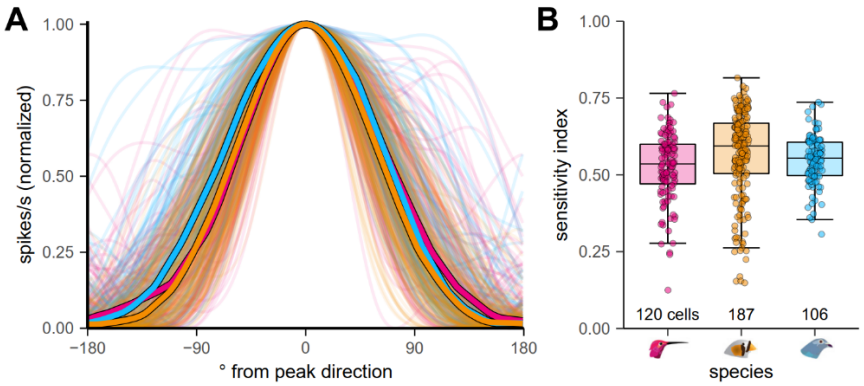

Figure S1. Directional tuning width of LM neurons of hummingbirds, zebra finches, and pigeons is similar, related to Figure 1. A) Tuning width was visualized by aligning the peaks of the normalized LM direction tuning curves. Thin lines are individual cells, which have been aligned at the direction that had the maximum firing rate. Thick lines indicate median values. B) Tuning width was analyzed by calculating the Sensitivity Index (SI), which measures the magnitude of the mean vector of the tuning curve[S1]. A neuron that responds to only one direction will have an SI value of 1, whereas a neuron responding equally to all directions has an SI value of 0. SI values are displayed in quartile box plots, with individual cells shown as circles. Overall, the neurons were broadly tuned for direction, with mean SI values ranging from 0.53 to 0.63. There were no differences in SI values among the three species. Hummingbird cells are indicated in magenta. Zebra finch cells are indicated in orange. Pigeon cells are indicated in blue.

Table S1. Mean values for model effects, with 5-95% credible intervals in parentheses. Each row corresponds to a separate model, related to Figure 2. Column 1 provides model formula. Abbreviations: SF – spatial frequency; TF – temporal frequency; LM – lentiformis mesencephali

Model	log2(spatial frequency):species			log2(temporal frequency):species		
	Hummingbird	Zebra Finch	Pigeon	Hummingbird	Zebra Finch	Pigeon
{SF, TF} ~ species	-3.96 (-4.25 – -3.62)	-2.55 (-2.89 – -2.23)	-2.11 (-2.44 – -1.76)	1.33 (1.01 – 1.64)	0.86 (0.55 – 1.15)	0.50 (0.15 – 0.82)

Model	Hummingbird	Zebra Finch	Pigeon
log2(velocity) ~ species	5.29 (4.77 – 5.80)	3.42 (2.88 – 3.91)	2.61 (2.07 – 3.18)

Table S2. Mean values for model effects, with 5-95% credible intervals in parentheses, related to Figure 3. Abbreviations: R_{vel} – partial correlation of velocity-oriented model; R_{ind} – partial correlation of spatiotemporally-independent model; LM – lentiformis mesencephali

Model	R_{vel}:species			R_{ind}:species		
	Hummingbird	Zebra Finch	Pigeon	Hummingbird	Zebra Finch	Pigeon
{R_{vel}, R_{ind}} ~ species	0.32 (0.26 – 0.38)	0.48 (0.42 – 0.55)	0.15 (0.07 – 0.21)	0.50 (0.44 – 0.56)	0.38 (0.33 – 0.45)	0.56 (0.49 – 0.63)

Supplemental References

S1. Vogels, R., and Orban, G.A. (1994). Activity of inferior temporal neurons during orientation discrimination with successively presented gratings. J Neurophysiol *71*, 1428–1451.